

## **IN-SPACE CHEMICAL PROPULSION**

### **SYSTEM MODEL**

**David C. Byers**

Science Applications International Corporation,  
Torrance, CA 90505

**Gordon Woodcock**

Gray Research,  
Huntsville, AL 35806

**Michael P.J. Benfield**

Science Applications International Corporation,  
Huntsville, Alabama, 35806

*The work described in this paper was funded in whole or in part by the In-Space Propulsion Technology Program, which is managed by NASA's Science Mission Directorate in Washington, D.C., and implemented by the In-Space Propulsion Technology Office at Marshall Space Flight Center in Huntsville, Ala. The program objective is to develop in-space propulsion technologies that can enable or benefit near and mid-term NASA space science missions by significantly reducing cost, mass or travel times.*

# IN-SPACE CHEMICAL PROPULSION SYSTEM MODEL

David C. Byers<sup>(1)</sup>, Gordon Woodcock<sup>(2)</sup>, M. P. J. Benfield<sup>(3)</sup>

<sup>(1)</sup>SAIC, 4465 Pacific Coast Hwy, Torrance, CA 90505 USA, byersdc@aol.com

<sup>(2)</sup>Gray Research, 655 Discovery Drive, Suite 300, Huntsville, AL 35806 USA, grw33@comcast.net

<sup>(3)</sup>SAIC, 675 Discovery Drive, Suite 300, Huntsville, AL 35806, michael.pj.benfield@saic.com

## ABSTRACT

Multiple, new technologies for chemical systems are becoming available and include high temperature rockets, very light propellant tanks and structures, new bipropellant and monopropellant options, lower mass propellant control components, and zero boil off subsystems. Such technologies offer promise of increasing the performance of in-space chemical propulsion for energetic space missions. A mass model for pressure-fed, Earth and space-storable, advanced chemical propulsion systems (ACPS) was developed in support of the NASA MSFC In-Space Propulsion Program. Data from flight systems and studies defined baseline system architectures and subsystems and analyses were formulated for parametric scaling relationships for all ACPS subsystems. The paper will first provide summary descriptions of the approaches used for the systems and the subsystems and then present selected analyses to illustrate use of the model for missions with characteristics of current interest.

## 1. REFERENCE SYSTEMS

The overall approach is shown in Fig. 1.

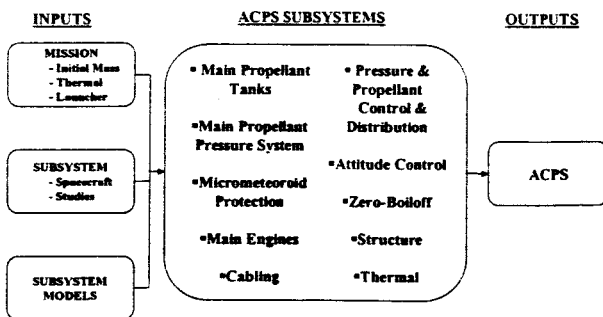


Fig. 1 ACPS model approach

Key mission inputs were obtained from detailed studies of missions of interest and included the propellant mass, obtained from mission energies and assumed rocket specific impulses, and thermal environments, which often included those of both deep space and inner planets (when gravity assist maneuvers were assumed). Missions and studies used for definitions ACPS architectures and baseline subsystem characteristics included the AXAF-I [1,2], a recent study of planetary stages that used cryogenic oxidizers

and storable fuels [3], Cassini [4,5], and review of planetary spacecraft by the Lockheed-Martin Corp. [6]. Major assumptions for all analyses included the use of Earth or space-storable (soft cryogenic) propellants and pressure-fed propellant tanks. Both bipropellant and monopropellant options were modeled. Subsequent studies will include deep cryogenic and pump-fed options but they were beyond the present scope. The primary metric was the wet mass of the propulsion system which may be combined with models of the remainder of the spacecraft and launch vehicle characteristics to predict payloads as a function of ACPS technologies.

## 2. REFERENCE SUBSYSTEMS

### 2.1 Main Propellant Tanks

Both composite overwrapped (CO) and metallic propellant tank options were modeled and, following [3] spherical tanks were assumed. The only large CO propellant tanks flown at the time of the writing were those on the AXAF-I [1]. The CO ACPS tanks were first scaled from AXAF-I by taking into account the change to spherical shape and the resultant changes in composite stresses. The baseline CO tanks also used the same areal mass densities of the composites, liners, and propellant management devices (PMDs) [7] of the AXAF-I propellant tanks. Those three tank elements were independently scaled via use of variable composite strengths and thickness (assumed to vary linearly with tank pressure), different liner thickness and materials, and adjustable PMD areal mass densities. Options for variable areal mass densities of both foam and multilayer insulation (MLI) were also included to allow appropriate [3,8] accommodation of mission (space and ground) thermal environments and propellant storage requirements. The propellant tank pressure was set by variable assumptions of main engine chamber pressure and pressure drops between the engine chamber and the propellant tank. Overall CO tank masses could then be calculated with variable values of propellant tank pressure (scaled from the baseline value of  $2.07 \cdot 10^6$  Pa), propellant mass, propellant tank volumes (which accounted for selectable values of propellant reserves, ullage, residuals, and assumed PMD volumes), and assumed mission thermal characteristics. Spherical metallic tank

masses, that included PMDs, were calculated directly from a manufacturer's database [9] and were adjusted to account for different propellant pressures and assumed foam and MLI layers.

## 2.2 Propellant Pressurization

Separate helium pressure subsystems were assumed for the fuels and oxidizers to avoid issues with long-term hypergolic propellant leakage and to allow for alternate pressurization approaches for individual propellants. The spherical helium propellant tanks were assumed, as in [10, 11] to be adjacent to, and at the same temperatures as, the associated propellant tanks. The AXAF-I helium tank, at a pressure of  $3.1 \cdot 10^7 \text{ Pa}$ , was taken as the baseline and for scaling purposes variable values of composite strength and liner thickness were assumed. The mass of the helium required for individual propellants was then calculated by consideration of the relevant propellant tank volumes, thermal environment, helium compressibility [12], MLI protection, and end-of-mission pressure drops between the propellant and pressure tanks (primarily in the regulator). Helium solubility was not included as it was judged to be a relatively small effect. For example, less than 2 percent of the loaded helium was dissolved into the Cassini propellants after 5 years of flight [4]. The mass of the helium tanks was then calculated as a function of the cited parameters. As discussed later, the mass of the helium pressurization systems penalizes the space-storable propellant options. Warm gas pressurization concepts [13,14] may mitigate that penalty, but multiple open issues exist [13] that must be addressed for long-term applications and that approach was not included herein. Consideration of warm gas pressurization is recommended, however, if research indicates it is viable for planetary-class missions.

## 2.3 Micrometeoroid Protection

It was recognized that micrometeoroid protection may be a requirement for some missions, in particular those that use both radioisotopes and Earth gravity assists and/or missions that involve traverses of regions with high micrometeoroids fluxes. However, no analyses were available of micrometeoroid protection masses which are extremely sensitive to specifics of spacecraft design. For those reasons, no masses were assumed for micrometeoroid protection, but it may be necessary to consider such penalties for selected missions and spacecraft configurations.

## 2.4 Main Engines

In these initial analyses, radiation-cooled and pressure-fed main engines were assumed. For generality, the

model included options for one or two main engines, but no penalty was taken for center-of-mass pointing. Following [3] and normal practice for planetary spacecraft, the thrust levels were assumed to be between 400 to 2000 N. That thrust range was felt to appropriately consider "gravity losses", deployed subsystems, and firing times typical of planetary missions and is similar to that of apogee propulsion for geosynchronous spacecraft. Both bipropellant and monopropellant options were included in the model. Rhenium bipropellant engines were assumed as they provide the highest performances available and versions tuned for MMH/NTO [15] and hydrazine/NTO [16] propellants have been flown and qualified, respectively. Rhenium engines are also compatible [17] with some of the fluorine-containing oxidizers of potential interest. Thruster masses were taken from historical data, modified to account for the assumed rhenium material and masses of heat shields and thruster mounts were scaled from [2]. Thrust chamber pressures were assumed to vary from  $6.9 \cdot 10^6$  to  $3.4 \cdot 10^6 \text{ Pa}$  and the composite overwrap of the propellant tank and the helium gas and tank masses were adjusted to accommodate the associated changes in propellant tank pressures. Bipropellant, main engine performances were calculated using state-of-art codes as functions of propellant options, thrust chamber pressure, mixture ratio, and thrust level. Bipropellant engine performance estimates were obtained state-of-art analyses [18] and data [16,19,20]. Values of advanced monopropellant performance and liquid characteristics were obtained directly from [21] and engineering estimates.

## 2.5 Pressure and Propellant Control/Distributions

The masses of the elements for control and distribution of the pressurants and propellants for the main engines are not negligible and were separately modeled. For convenience, the control and distribution subsystem was divided into "legs" with a leg being defined as any connection between a pressure and propellant tank or between a propellant tank and a thruster. For example, monopropellant and bipropellant options with two main engines would have three and six "legs", respectively. The pressurant and propellant control and distribution components included, respectively, valves, regulators, filters, and etc. and lines, fittings, brackets, and MLI and heaters associated with propellant lines. The number and type of control components was taken directly from [4] (with minor exceptions that were consistent with use of separate pressure tanks and Venturi valves). The masses of the control components for both Earth and space-storable propellant options were taken from [22] (except for Venturi valves and trim orifices whose masses were estimated). Components for space-storable propellants were

typically heavier than those for Earth-storable options. The mass of the distribution "legs" were scaled directly from [1,2] where the mass was also scaled with the linear dimension of the ACPS which was assumed proportional to the cube root of the total propellant load.

## 2.6 Attitude Control Subsystem (ACS)

A separate ACS that used hydrazine propellant was assumed for all cases. The required hydrazine propellant mass is extremely mission dependent, but was set as the same fraction of initial spacecraft mass as used for Cassini [5]. The number and type of thrusters and pressurant and propellant control components for the ACS were taken from [4,5]. Masses of the spherical propellant tanks were set as a fraction of the ACS propellant mass derived from a straight-line plot of the values on AXAF-I [1] and Cassini [5]. The mass of the distribution elements was taken from AXAF-I data modified to account for the different number of thrusters on Cassini.

## 2.7 Zero Boiloff (ZBO)

ZBO was assumed for thermal control for all space-storable propellants. This approach was taken as a very detailed study [23] indicated that passive storage of fluorine, a typical space-storable propellant, for an outbound planetary mission required major deviations from normal spacecraft designs. Also, as will be seen, ZBO can be implemented for space-storable propellants with relatively small power and mass penalties. The ZBO subsystem comprised the cryocooler, control electronics, a radiator for the control electronics, and the additional power required. The overall modeling approach was to determine the ZBO powers and masses as functions of the cold head temperature of the cryocooler, required cooling power, the environmental temperature of the spacecraft. The cold head temperature was assumed to be 80K for all space-storable propellants. This had the effect of slightly penalizing the warmer options, but did allow for temperature drops experienced with practical cryocoolers [8]. The cooling power and environmental temperatures are very dependent on mission and spacecraft design and were treated as inputs for specific missions. The ZBO input power was obtained using the global approach of [8] (which accounts for the rejection temperature of the radiator), along with cryocooler specific powers from [24], and the power control electronics efficiency recommended by [25]. Total ZBO mass was the sum of the cryocooler (modeled as a function of cooling power and cold head temperature in [24]), the control electronics (obtained from the lowest values of power processor specific

mass in [25]), the radiator (using the model of areal mass vs radiated power for a beryllium radiator from [26]), and a mass to account for the input power requirement. A small mass was also added to account for a cooling loop to be used during ground operations.

## 2.8 Thermal, Cabling, and Structure

Secondary structure was defined as the supports for the propellant and pressurant tank and was modeled as a function of main propellant mass from data available for several spacecraft [6]. Elements sometimes counted as secondary structure were accounted for in the pressurant and propellant distribution allocations cited above. Primary structure supported the ACPS, connected the launch vehicle adapters to the payload, and supported launch loads. The primary structure was found to be significant and was taken from a plot of the ratio of the primary structure to initial masses of several, recent planetary spacecraft [6]. To account for linear dimensions of different ACPS, cabling masses were calculated by multiplying the AXAF-I propulsion cable mass by the ratio of the cube roots of the total propellant masses of the ACPS and AXAF-I. Thermal masses for propellant tanks and propellant distribution subsystems were previously discussed. Following [3], 13 layers of MLI were taken to cover the outer primary structure which, for scaling purposes was assumed to be a cylinder with a diameter and length slightly larger, respectively, than the diameter of the largest propellant tank and sum of diameters of all propellant tanks. The MLI was scaled for all applications herein, by using the data of [27] for the average mass per unit area and layer of variable density MLI.

## 3. SELECTED ACPS MODEL OUTPUTS

This section will provide some initial examples of the use of the ACPS model. Only the characteristics of the ACPS will be discussed herein; but the results can be straightforwardly used to define payloads via combination with specific inputs regarding missions, launchers, and other spacecraft subsystems.

Figs. 2 and 3 show the wet and dry masses, respectively, of monopropellant, Earth-storable (NTO/N<sub>2</sub>H<sub>4</sub>) and space-storable (LO<sub>x</sub>/N<sub>2</sub>H<sub>4</sub>) ACPS for a mission with an initial mass and delta V, respectively, of 3000kg and 2500 m/sec. The specific impulses of the monopropellant and LO<sub>x</sub>/N<sub>2</sub>H<sub>4</sub> options have been demonstrated in short term tests and the performance with NTO/N<sub>2</sub>H<sub>4</sub> is representative of a qualified engine. The LO<sub>x</sub>/N<sub>2</sub>H<sub>4</sub> option did not provide a mission benefit proportional to its specific impulse as the dry mass was penalized by oxidizer leg requirements for additional helium, more layers of MLI, heavier propellant distribution and control components. The ZBO mass

for this representative space-storable is quite modest which suggests that approach may be generally optimal for 80 K- class propellants. One potential additional benefit from use of ZBO may be the avoidance of very mission specific spacecraft designs, which were found necessary in prior detailed analyses of fluorine propulsion [23].

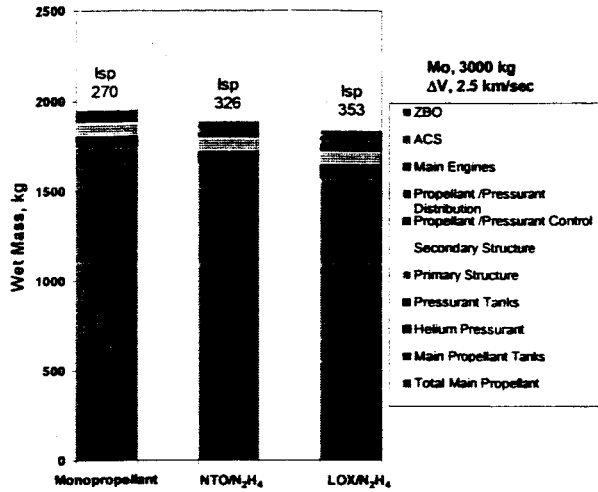


Fig. 2 ACPS wet mass vs propellant option

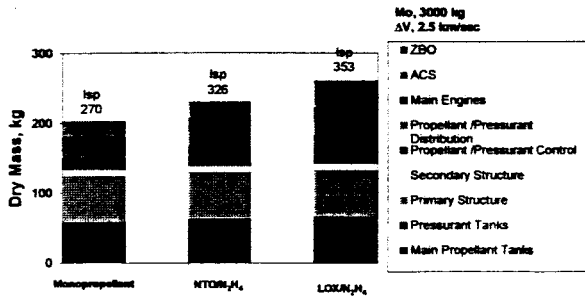


Fig. 3 ACPS dry mass vs propellant option

Figs. 4 and 5 show ACPS wet and dry masses, respectively, for the NTO/N<sub>2</sub>H<sub>4</sub> option vs chamber pressure ( $P_c$ ) with CO propellant tank and mixture ratio (MR) options. Operation at higher than normal chamber pressures didn't offer much benefit, even with light weight propellant tanks (which assumed liner thickness' of ~ 0.13mm and a 2x increase in composite strength over the baseline). This occurred as the increased masses of the pressurant subsystem and the propellant tanks overcame the increases in main engine performance. However, substantial reductions in ACPS wet mass are offered by both advanced propellant tanks and higher MR operation at nominal values of  $P_c$ . Operation at increased MR does imply, however, higher temperature combustion and wall temperatures than have been demonstrated for long terms with qualified rhenium engines [15, 16]. It is noted that

higher thrust levels than the assume 445N may offer benefits via reduced operating times and delta v's for some applications in gravity wells.

ACPS wet masses for advanced monopropellants and state-of-art Earth-storable bipropellants are shown in Fig. 6 for a range of mission options. It is seen that, for low energy missions, the advanced monopropellant options have masses about equal to those of the baseline bipropellant approach. It is possible that such monopropellants could provide significant hardware and ground management cost benefits for selected missions due to reduced system complexity and, in some cases, toxicity.

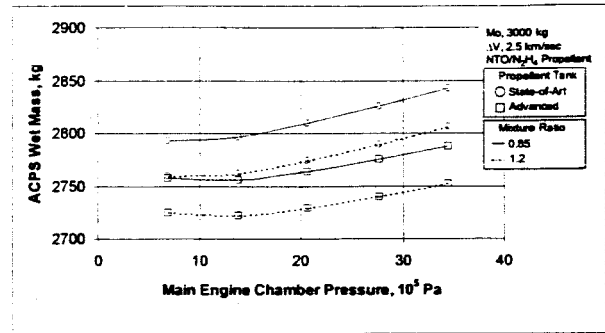


Fig. 4 ACPS wet masses vs  $P_c$ , MR, and tank options

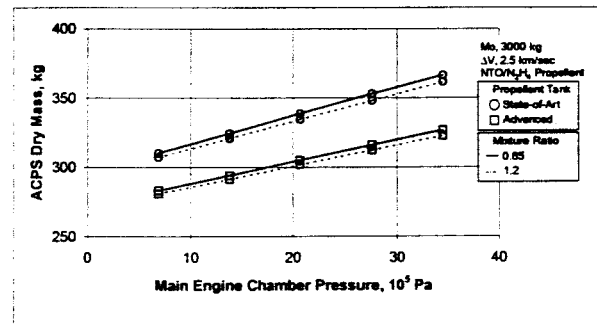


Fig. 5 ACPS dry masses vs  $P_c$ , MR, and tank options

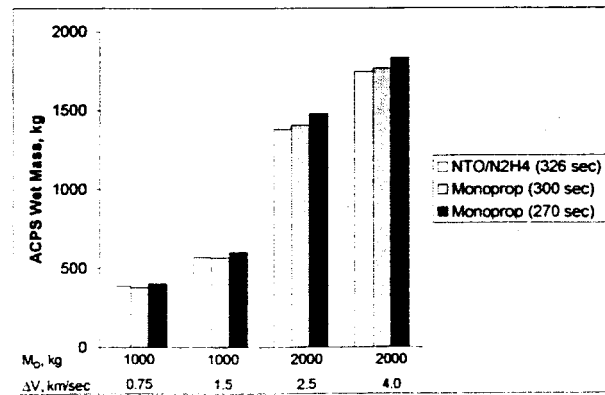


Fig. 6 ACPS wet masses vs missions and propellant

An example of the effect of mission thermal environment is shown in Fig. 7 where the mass of the ZBO subsystem for LO<sub>x</sub> plotted as a function of the hottest environmental temperature assumed for a mission. In these analyses, the thermal environment affected both the efficiency of the cryocoolers and the mass of the radiator for the control electronics. The thermal heat leaks were constant for the data of Fig. 7 but will be considered as a variable in the future. The thermal environments were taken from [28] with hottest temperatures of 328K and 448K being associated with Venus and Mercury, respectively. It is seen that the ZBO masses remained relatively low, except for the extreme environment near Mercury.

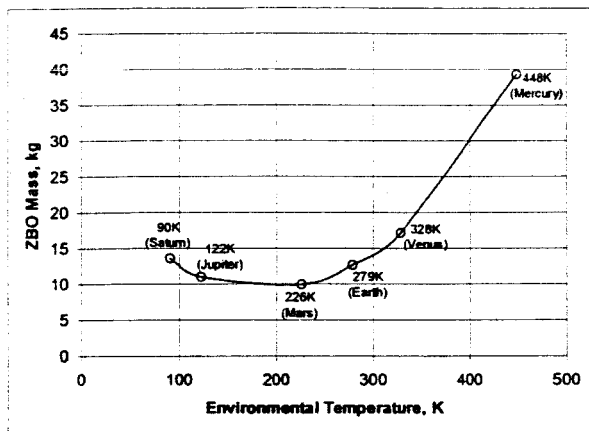


Fig. 7 ZBO masses vs environmental temperature

#### 4. CONCLUDING REMARKS

A flexible model for ACPS has been developed that enables quick evaluations of different technology options and global mission characteristics. Updates may be easily implemented as new findings become available. Examples of use of the model were presented that illustrated the sensitivity of ACPS mass to a variety of advanced technologies and mission energies, initial masses, and thermal environments.

#### 5. REFERENCES

- Mayer, N. L., Advanced X-ray Astrophysics Facility-Imaging (AXAF-I) Propulsion Subsystem, AIAA 96-2869, 32<sup>nd</sup> AIAA/ASME/SAE/ASEE Joint Propulsion Conference & Exhibit, Lake Buena Vista, FL., 1996.
- NASA DPD692 SE09, Advanced X-ray Astrophysics Facility Mass Properties Report, March, 1999.
- Honda, L., Calvignac, J., and Matuszak, L., Storable Thruster Technology Program-Mission Study, The 2002 JANNAF Propulsion Meeting, 2002.
- Barber, T. J. and Cowley, R. T., Initial Cassini Propulsion System In-flight Characterization, AIAA 2002-4152, 38<sup>th</sup> AIAA/ASME/SAE/ASEE Joint Propulsion Conference & Exhibit, Indianapolis, IN., 2002.
- Leeds, M. W., Eberhardt, R. N., and Berry, R. L., Development of the Cassini Spacecraft Propulsion Subsystem, AIAA 96-2864, 32<sup>nd</sup> AIAA/ASME/SAE/ASEE Joint Propulsion Conference & Exhibit, Lake Buena Vista, FL., 1996.
- Personal Communication, Gamber, T., Lockheed Martin Corporation, January, 2004.
- Personal Communication, C. Murray, General Dynamics Technical Division, Lincoln Operations, March, 2003.
- Plachta, D. and Kittel, P., An Updated Zero Boil-off Cryogenic Propellant Storage Analysis Applied to Upper Stages of Depots in an LEO Environment, AIAA 2002-3589, 38<sup>th</sup> AIAA/ASME/SAE/ASEE Joint Propulsion Conference & Exhibit, Indianapolis, IN., 2002.
- [http://www.psi-pci.com/Data\\_Sheet\\_Index\\_PMD-VOL.htm](http://www.psi-pci.com/Data_Sheet_Index_PMD-VOL.htm), Pressure Systems Inc., March, 2004.
- Meissinger, H. F., Davenport, W. L., and Dugan, D. W., Advanced Bipropellant Systems for Use on Planetary Orbiters, AIAA Paper No. 75-1190, AIAA/SAE 11<sup>th</sup> Propulsion Conference, Anaheim, CA, 1975.
- Bond, D. L., Appel, M. A., and Kruger, G. W., Fluorine-Hydrazine Propulsion Technology Update, The 1980 JANNAF Propulsion Meeting, Vol. 5, 147-164, 1980.
- Sychev, V. V. et al., *Thermodynamic Properties of Helium, National Standard Reference*, Hemisphere Publishing Corp., Washington D. C., 1987.
- Guernsey, C. S., Mars Ascent Propulsion Systems (MAPS) Technology Program: Plans and Progress, AIAA 98-3664, 34<sup>th</sup> AIAA/ASME/SAE/ASEE Joint Propulsion Conference & Exhibit, Cleveland, OH, 1998.
- Reed, B. D., Jankovsky, R. S., and McGuire, T. J., Testing of a 2.2-N Triconstituent Gas Thruster, AIAA-3668, 34<sup>th</sup> AIAA/ASME/SAE/ASEE Joint Propulsion Conference & Exhibit, Cleveland, OH, 1998.
- Wu, P.-K., et al., Qualification Testing of a 2<sup>nd</sup> Generation High Performance Apogee Thruster, AIAA 2001-3253, 37<sup>th</sup> AIAA/ASME/SAE/ASEE Joint Propulsion Conference & Exhibit Salt Lake City, UT, 2001.
- Krimer, D., et al., Qualification Testing of a High Performance Bipropellant Rocket Engine Using MON-3 and Hydrazine, AIAA 2003-4775, 39<sup>th</sup> AIAA/ASME/SAE/ASEE Joint Propulsion Conference & Exhibit, Huntsville, AL, 2003.
- Appel, M. A., Kaplan, R. B., and Tuffias, R. H., Liquid Fluorine/Hydrazine Rhenium Thruster Update, The 1983 JANNAF Propulsion Meeting, Vol. 1, 85-90, 1983.

18. Personal Communication, Lu, F., Aerojet General Corporation, 2004.
- 19 Chazen, M. L., et al. High Pressure, Earth Storable Rocket Technology Program HIPES-Basic Program Final Report, NASA CR 195449, March, 1995.
- 20 Jassowski, D. M., High Pressure, Earth-Storable Rocket Technology, Vol. 1, NASA CR 195427/Vol. 3, 1997.
- 21, Personal Communication, Myers, R. M., Aerojet General Corporation, 2004.
22. Schneider, S. J., On-Board Propulsion System Analysis of High Density Propellants, AIAA 98-3670, 34<sup>th</sup> AIAA/SAME/SAE/ASEE Joint Propulsion Conference & Exhibit, Cleveland, OH, 1998.
23. Stultz, J. W. and Grippi, R. A., A Summary and Update of the Configuration and Temperature Control Studies for a Fluorine-Hydrazine Propulsion System, The 1979 JANNAF Propulsion Meeting, Vol. 1, 529-555, 1979.
24. ter Brake, H. J. M. and Wiegerinck, G. G. M., Low-power Cryocooler Survey, *Cryogenics*, 42, 705-718, 2002.
25. Glaister, D. S, Donabedian, M., Curran, D. G. T., and Davis, T., An Assessment of the State of Cryocooler Technology for Space Applications, The Aerospace Corporation, Report No. TOR-98 (1057)-3, 1998.
26. Juhasz, A. J., Tew, R. C., and Thieme, L. G., Parametric Study of Radiator Concepts for a Stirling Radioisotope Power System Applicable to Deep Space Missions, NASA/TP-2000-209676, 2000.
27. Hastings, L. J. and Martin, J. J., Experimental Testing of a Foam/Multilayer Insulation (FMLI) Thermal Control System (TCS) for Use on a Cryogenic Upper Stage, Space Technology and Applications International Forum, 331-341, 1998.
28. Juhasz, A. J., An Analysis and Procedure for Determining Space Environmental Sink Temperatures with Selected Computational Results, Proceedings of the Intersociety Energy Conversion Engineering Conference, Vol. 2, 1175-1183, 2000.